



BNL-212080-2019-TECH

NSLSII-ASD-TN-314

## APS-U Bellows/BPM Assembly Test in NSLS-II

A. Blednykh

August 2019

Photon Sciences

**Brookhaven National Laboratory**

**U.S. Department of Energy**

USDOE Office of Science (SC), Basic Energy Sciences (BES) (SC-22)

Notice: This technical note has been authored by employees of Brookhaven Science Associates, LLC under Contract No. DE-SC0012704 with the U.S. Department of Energy. The publisher by accepting the technical note for publication acknowledges that the United States Government retains a non-exclusive, paid-up, irrevocable, world-wide license to publish or reproduce the published form of this technical note, or allow others to do so, for United States Government purposes.

## **DISCLAIMER**

This report was prepared as an account of work sponsored by an agency of the United States Government. Neither the United States Government nor any agency thereof, nor any of their employees, nor any of their contractors, subcontractors, or their employees, makes any warranty, express or implied, or assumes any legal liability or responsibility for the accuracy, completeness, or any third party's use or the results of such use of any information, apparatus, product, or process disclosed, or represents that its use would not infringe privately owned rights. Reference herein to any specific commercial product, process, or service by trade name, trademark, manufacturer, or otherwise, does not necessarily constitute or imply its endorsement, recommendation, or favoring by the United States Government or any agency thereof or its contractors or subcontractors. The views and opinions of authors expressed herein do not necessarily state or reflect those of the United States Government or any agency thereof.

<b>NSLS-II TECHNICAL NOTE</b> <b>BROOKHAVEN NATIONAL LABORATORY</b>	<b>NUMBER</b> <b>NSLSII-ASD-TN-314</b>
<b>AUTHORS</b> A. Blednykh, B. Bacha, G. Bassi, L. Doom, C. Hetzel, R. Fliller, D. Padrazo, S. Sharma, V. Smaluk, R. Smith, T. Shaftan, G. Wang, G. Fries	<b>DATE</b> 08/05/2019
<i><b>APS-U Bellows/BPM Assembly Test in NSLS-II</b></i>	

## APS-U Bellows/BPM Assembly Test in NSLS-II

### Aug. 5, 2019

A. Blednykh, B. Bacha, G. Bassi, L. Doom, C. Hetzel, R. Fliller, D. Padrazo, S. Sharma, V. Smaluk,  
R. Smith, T. Shaftan, G. Wang, G. Fries  
Brookhaven National Laboratory, Upton, NY, U.S.A.

#### Abstract

We report on beam studies performed at NSLS-II to test the performance of the APS-U Bellows/BPM assembly.

## 1. Introduction

The beam studies have been performed with the following machine parameters: lattice with three Damping Wigglers (3DWs) magnet gap closed and the RF voltage  $V_{RF} = 3MV$ , energy spread  $\sigma_{\delta o} = 8.2 \times 10^{-4}$  and a bunch length of  $\sigma_s = 4.4mm$ . The RF voltage was not changed during any of the performed studies, since the RF system was not optimized after the recent installation of the second cavity. The average current was increased in several steps during each shift,  $I_{av} = 2mA$ ,  $I_{av} = 25mA$ ,  $I_{av} = 50mA$ , ... The vacuum pressure trip limits on the near the tested APS-U assembly were not changed. The temperature interlock for the newly installed components were set to  $100^\circ C$ . In addition, an infrared (IR) camera was installed for the visual temperature monitoring in the area. The wide-angle view included the transition area as well as the APS-U Bellows/BPM assembly. All of the data was archived except for the IR camera images. Images from the IR camera were saved at different average current. An animated gif-file was created and sent out by e-mail to the APS-U team along with other interim results.

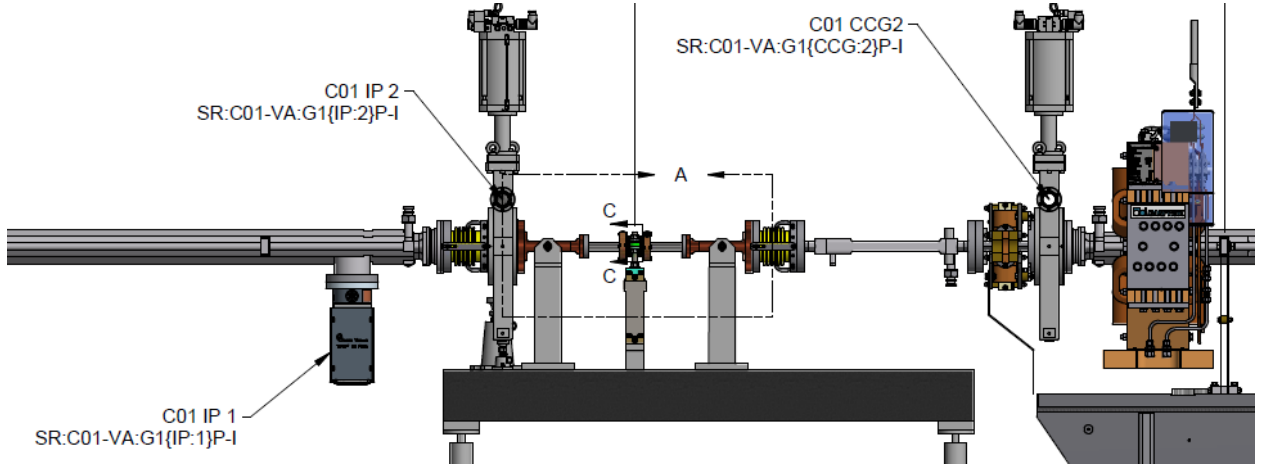


Fig. 1: Partial layout of the NSLS-II short straight section with extra gate valve and the APS-U Bellows/BPM assembly installed.

## 2. Power loss comparison for NSLS-II and APS-U

In Table 1, we present comparison of the main parameters for two accelerator facilities, NSLS-II and APS-U. The loss factor as a function of bunch length is presented in Fig. 2 for the model with the MPF BPM Button.

Table 1: Main Parameters of the APS-U and NSLS-II storage rings

Parameters	APS-U	NSLS-II
Average Current, $I_{av}$	200mA	400mA (100mA)
Number of Bunches, $M$	48	1050 (80% fill)
Revolution Period, $T_0$	3.682 $\mu s$	2.64 $\mu s$
Bunch Duration, $\sigma_s$ ignoring bunch lengthening	15mm	5mm (3DWs)
Power Loss, $P_{loss}$ $P_{loss} = \frac{k_{loss} I_{av}^2 T_0}{M}$	$P_{loss} = k_{loss} \times 306$ $= 0.5W$	$P_{loss} = k_{loss} \times 402$ $= 7W (0.5W)$

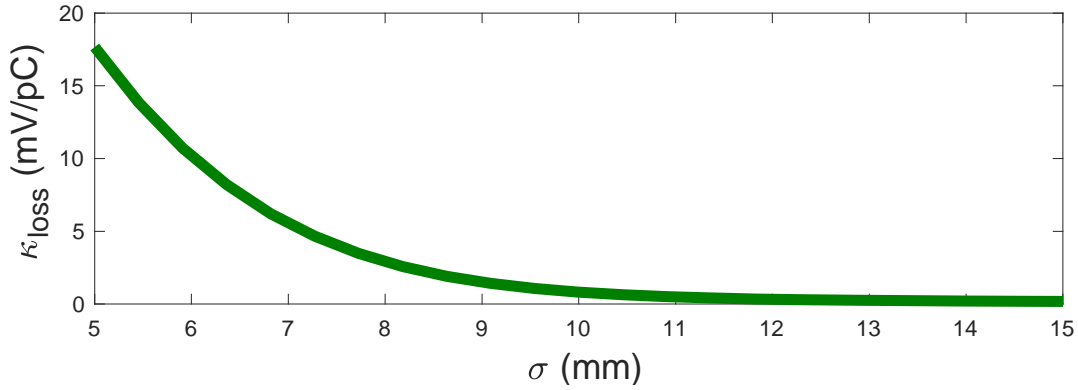


Fig. 2: The loss factor as a function of bunch length for the simplified APS-U bellows/BPM geometry.  $k_{loss}(15mm) = 0.17mV/pC$  and  $k_{loss}(5mm) = 18mV/pC$ .

To obtain the relevant power loss as the APS-U project, the NSLS-II should operate at  $I_{av} = 100mA$  within  $M = 1050$  bunches.

### 3. Beam Test

The APS-U Bellows/BPM Assembly was installed in the NSLS-II storage ring at the end of a short-straight section (Fig. 1). To match the APS-U chamber aperture, tapered transitions from the standard NSLS-II octagonal shape to the APS-U circular shape were installed with an additional gate valve (GV) to separate the test area from the rest of the storage ring. A total of ten RTDs (Fig. 3) were mounted at different locations on and near the APS-U Bellows/BPM assembly for the temperature monitoring. A sample image from the IR camera is shown in Fig. 4. For orientation, the electron beam is traveling from left to the right. It should be noted that RTD10 and RTD11 are affixed on the convolutions of the downstream and upstream bellows, respectively.

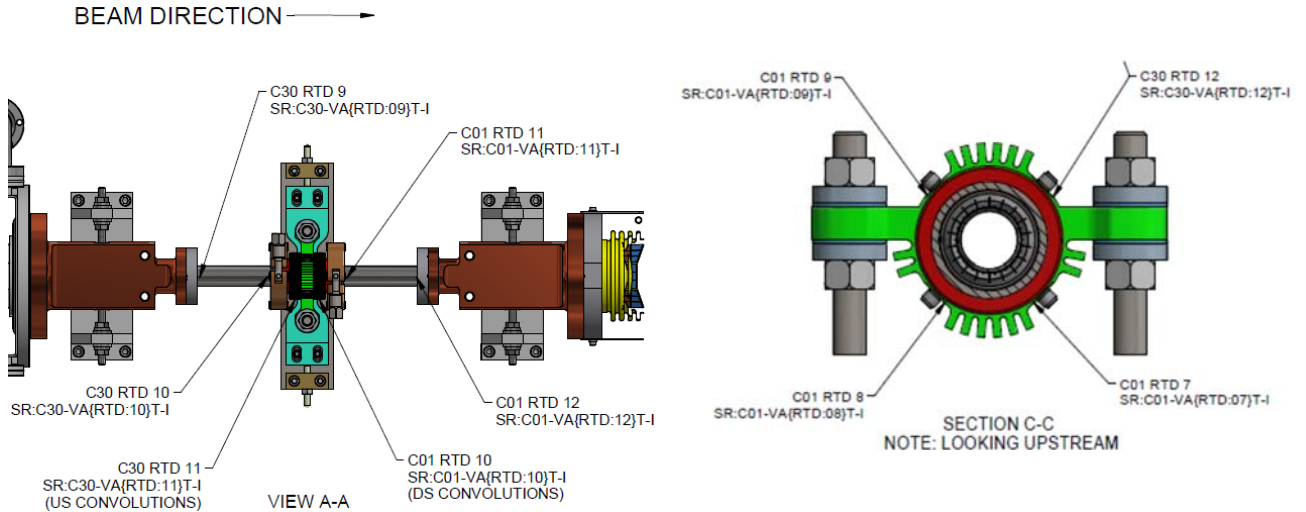


Fig. 3: The APS-U Bellows/BPM assembly with ten RTDs installed at different locations.

Two runs at high current,  $I_{av} \leq 100mA$ , separated by 24 hours, were performed to measure the temperature rise of the APS-U bellows. These test cycles will be referred to as Run1 and Run2. The results of the local temperature rise and the local vacuum pressure as a function of average current are shown in Fig. 5 (Aug. 2, 2019 – Run1) and in Fig. 6 (Aug. 3, 2019 – Run2). The temperature readings from all RTD's with an average current of 100mA during the Run1 show little change in temperature. At higher average currents, the difference in temperature between RTD11 and all other RTDs becomes apparent. At the same time, the thermal view of the IR camera shows the appearance of localized heating on the upstream side of the APS-U Bellows/BPM assembly. The IR camera image shown in Fig. 4 is with a stored beam current of  $I_{av} = 75mA$ . The beam was dumped due to the temperature interlock limit with  $I_{av} = 100mA$  (Fig. 5, dark wine trace of RTD11). None of the gate valves closed during this time and the vacuum pressure was normal after re-injecting beam into the ring. The data from Run2 is presented in Fig. 6. The same temperature behavior was observed on RTD11 during the average current increase. Figure 7 shows the temperature rise of RTD11 during Run1 at  $I_{av} = 100mA$  (blue trace) and Run2 at  $I_{av} = 86mA$  (green trace). The temperature rises during both runs show a similar behavior and can be characterized by three different regimes.

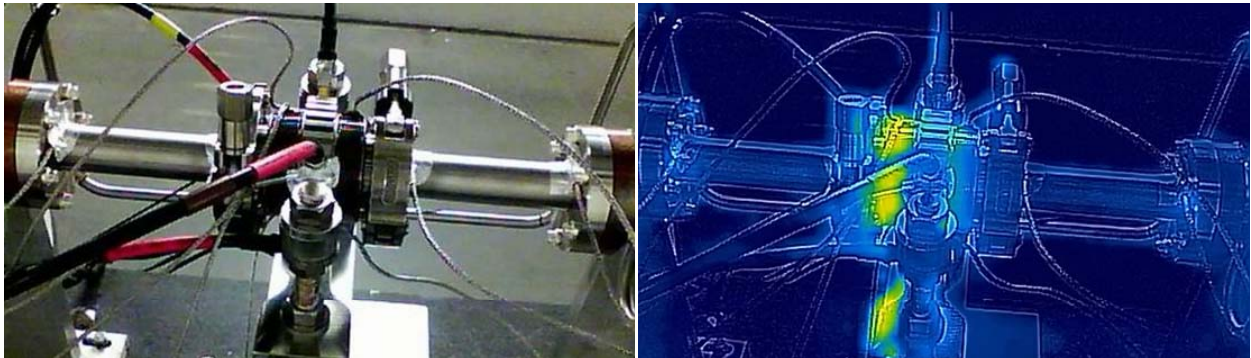


Fig. 4: IR camera view of the APS-U Bellows/BPM assembly (visible and IR spectrum)

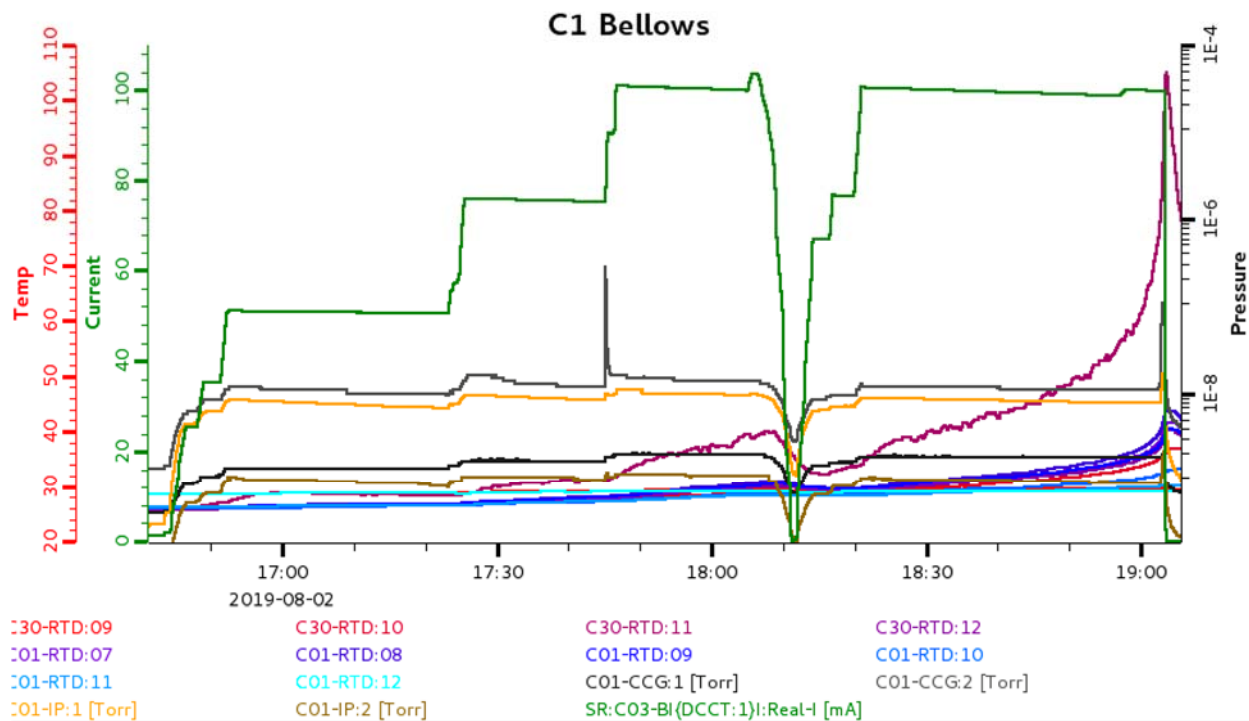


Fig. 5: The summary results of Run1

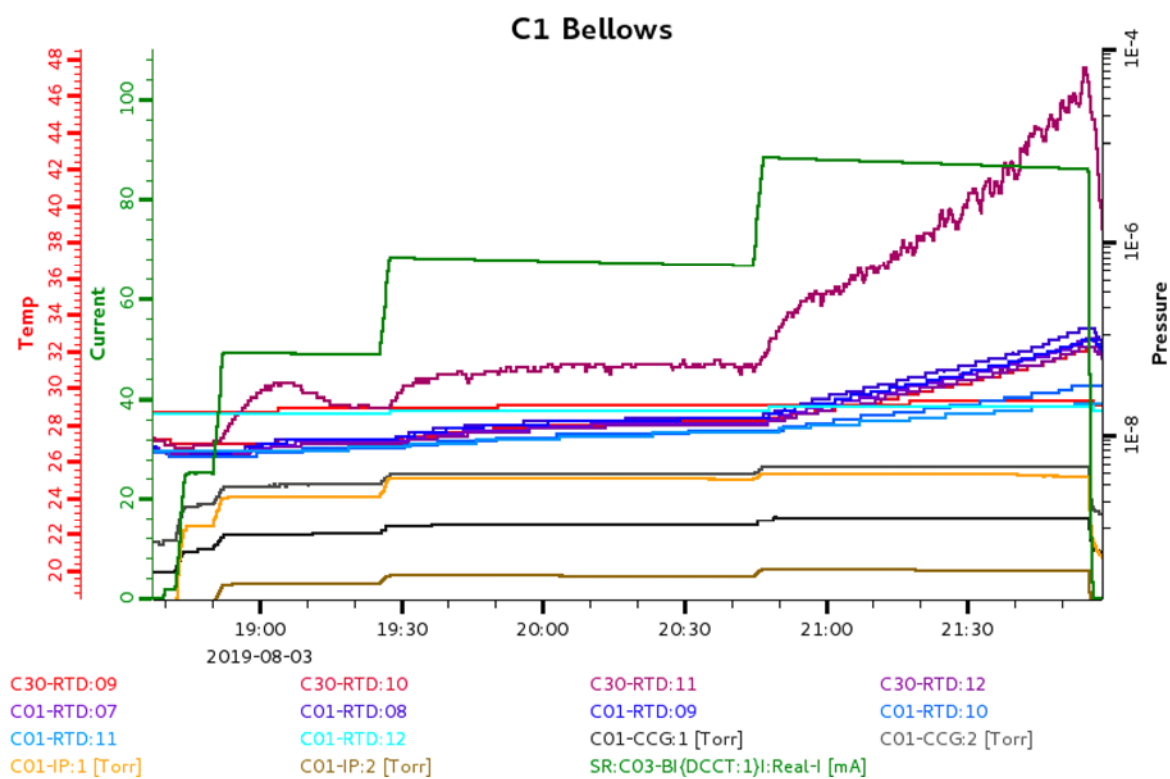


Fig. 6: The summary results of Run2

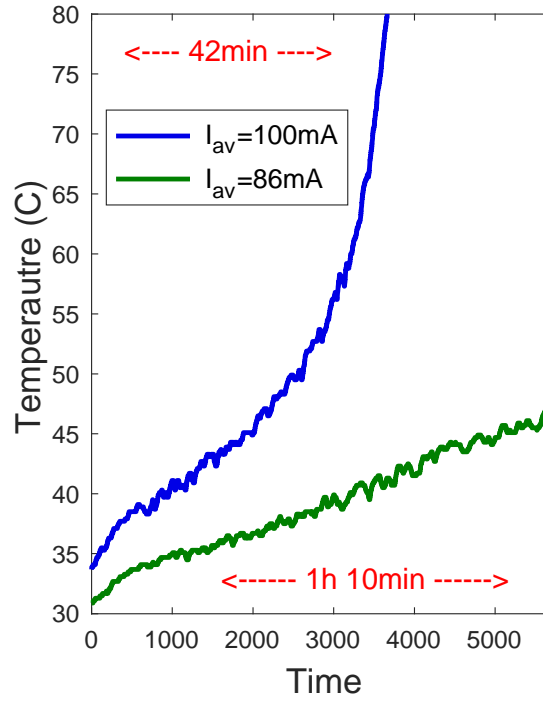


Fig. 7: Temperature rise vs. time measured by RTD11 at  $I_{av} = 100mA$  (blue trace) and  $I_{av} = 86mA$  (green trace)

In the first regime (Fig. 8a) the temperature reaches a steady-state condition after some period, while in the second regime (Fig. 8b) the temperature grows linearly from its steady state value as a response to local heating. In the third regime, the temperature shows an exponential growth (Fig. 8c). All three regimes were well fitted with the following formulas:

Steady State Regime:

$$T(t) = T_{max}(1 - aExp[-g(t - t_0)]),$$

$$t_0 \leq t \leq t_1$$

where  $T_{max} = 39^\circ C$  is the steady state temperature,  $a = 0.15^\circ C$  and  $g = 0.004s^{-1}$ .

Linear Regime:

$$T(t) = T_{max} + A(t - t_1),$$

$$t_1 \leq t \leq t_2,$$

where  $A = 0.005^\circ C/s$ .

Exponential Growth Regime:

$$T(t) = T(t_2) + bExp[d(t - t_2)],$$

$$t \geq t_2$$

where  $T(t_2) = 45^\circ C$ ,  $b = 1.37^\circ C$  and  $d = 0.002s^{-1}$ .



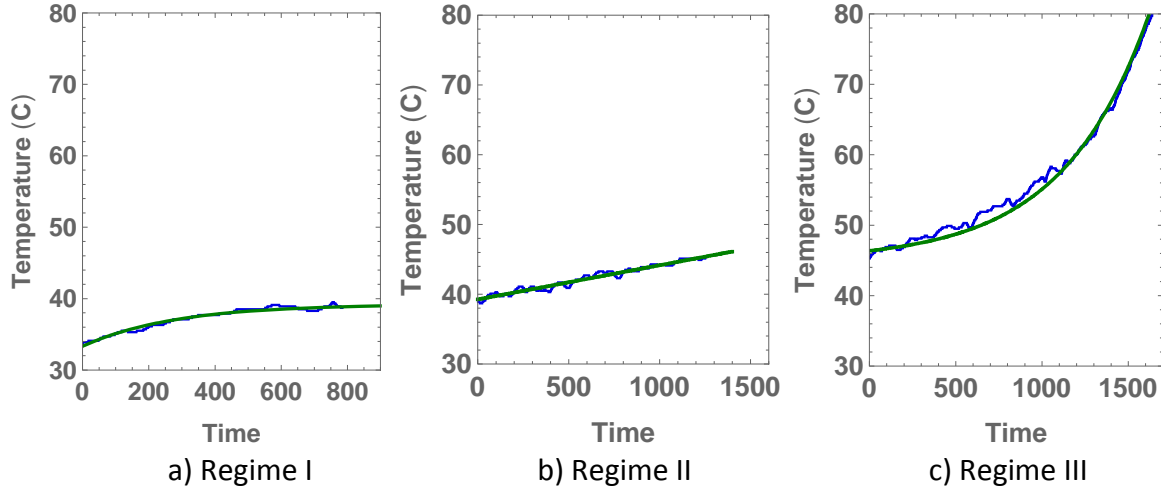


Fig. 8: Temperature rise separated by three different regimes. The blue traces are the experimental results of the temperature at different time. The green trace is the data fit.

In Fig. 9, the experimental data of the temperature for the steady-state condition are summarized as a function of average current  $T(I_{av})$ . The temperature has a quadratic dependence on  $I_{av}$ ,  $T \sim I_{av}^2$ . The results at high-current were not considered since the temperature did not reach the steady-state. Data from several of the RTDs showing a similar temperature response are plotted in Figure 9.

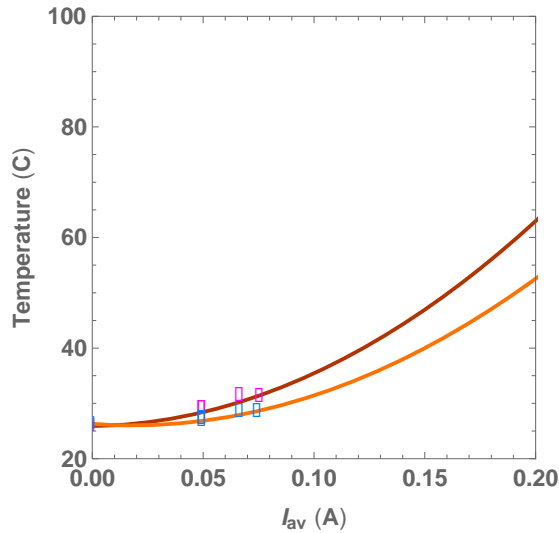


Fig. 9: Experimental data of the temperature collected for the APS-U Bellows/BPM within two beam study shifts at  $V_{RF} = 3MV$  with  $M = 1200$  bunches. Results at  $I_{av} = 86mA$  and  $I_{av} = 100mA$  were not included. The magenta dots are the temperature reading from RTD11 and the wine trace is the data fit. The blue dots are the temperature reading from RTD9 and the orange trace is the data fit.

The local heat which appears on the upstream side of the APS-U Bellows/BPM is because the upstream RF contact fingers were not being compressed against the central BPM body pipe (green colored in Fig. 10). There is only a nominal overlap of 2.6mm before the fingers fall off of the central body. The bellows were made 2.3 mm longer on each side inadvertently which could lead to poor contact between the RF contact fingers and the BPM wide, or even an axial gap between the two. Sharp temperature excursions at more than one circumferential location, which can be seen clearly in the infrared movie, suggest the latter possibility. The exponential temperature rise seen by RTD11 for the  $I_{av} = 100mA$  case may be related to changes in the upstream geometry amplifying poor contact or axial gap.

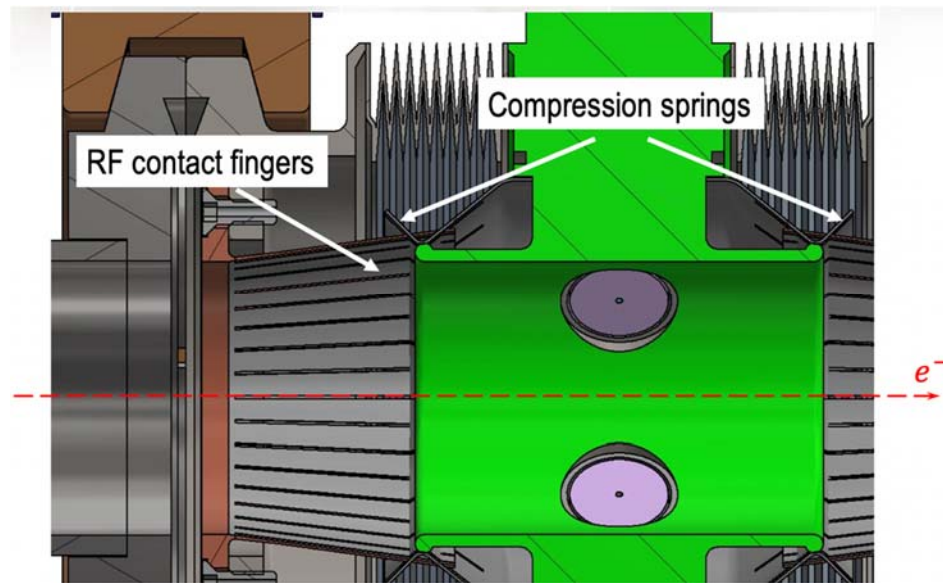


Fig. 10: The internal view of the APS-U Bellows/BPM assembly.

On Monday, August 5, 2019, the APS-U Bellows/BPM assembly was removed from the ring. The images of the internal part of the bellows including the view of the RF contact springs are shown in Fig. 11 and Fig. 12. Visual inspection revealed no evidence of the RF contact fingers burning, melting or deforming. As can be seen in the images, there is a gap between the RF fingers and the BPM body. This results in a situation where the electron beam 'sees' a large cavity structure where the electromagnetic fields can penetrate and generate resonance modes. Numerical simulations can be performed to confirm this scenario.

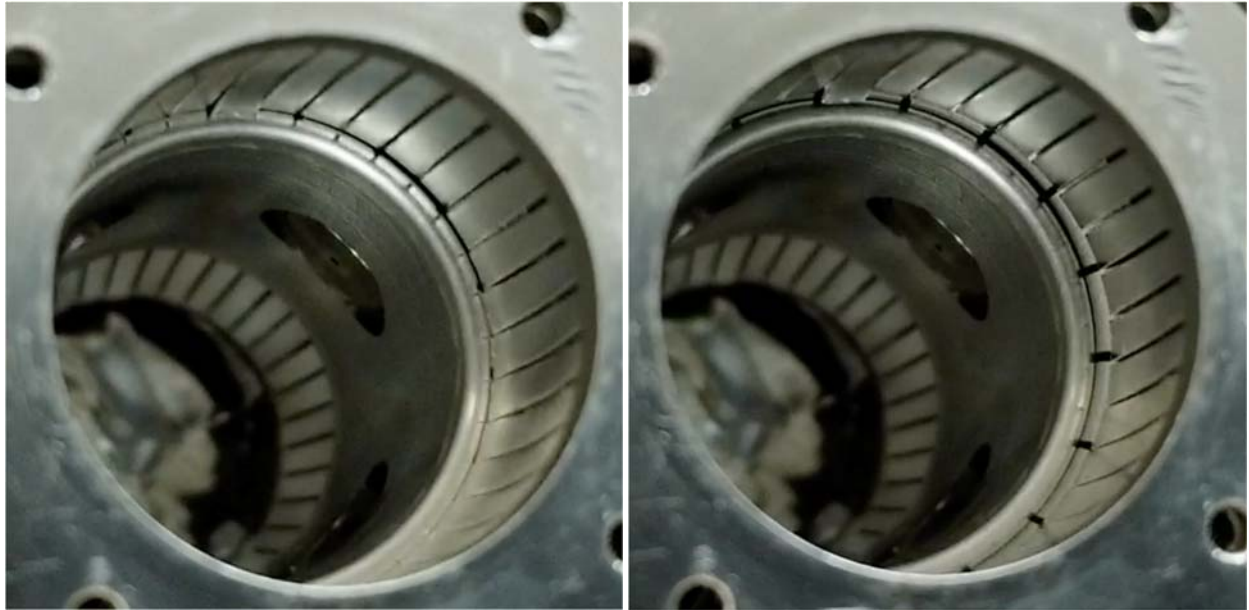


Fig. 11: The upstream side of the APS-U Bellows/BPM assembly view after its deinstallation from the ring. a) The RF contact fingers compressed manually towards the BPM pipe. b) The RF contact fingers in the uncompressed position.



Fig. 12: The upstream side of the APS-U bellows/BPM assembly after the beam test in NSLS-II with another angle of view. The RF contact fingers longitudinal compressed towards the BPM pipe.

A low-frequency resonance at  $f \sim 1.6\text{GHz}$  has been observed during beam spectra measurements directly from the BPM Button [Reference to the diagnostic group measurements]. The numerical analysis of the APS-U Bellows/BPM model with ideal contact of the RF contact fingers (Fig. 13) shows the appearance of longitudinal trapped mode due to the BPM Button geometry (Fig. 14 and Fig. 15). The MPF BPM Button housing was modified allowing the

electromagnetic field to penetrate through the ceramic washer where a trapped mode can be generated. The BPM design for the NSLS-II small aperture BPM button, also manufactured by the MPF company is shown in Fig. 16.

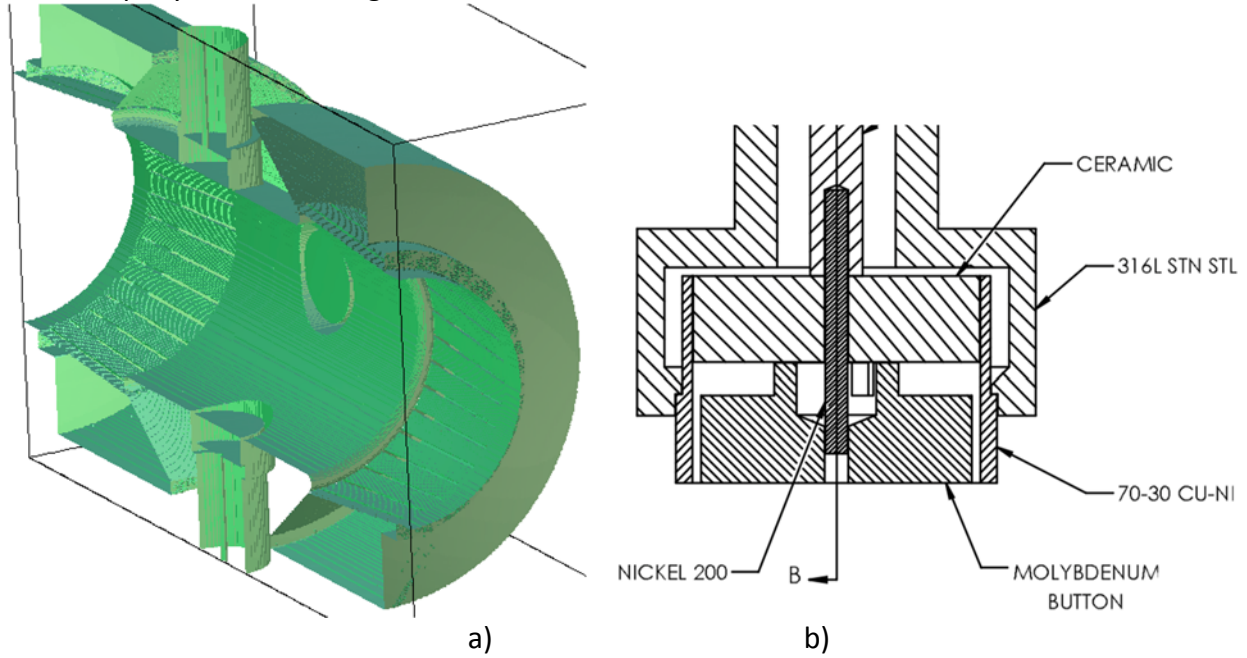


Fig. 13: APS-U Bellows/BPM assembly. a) Simplified model with BPM Button pins only. b) Final designed MPF BPM Button.

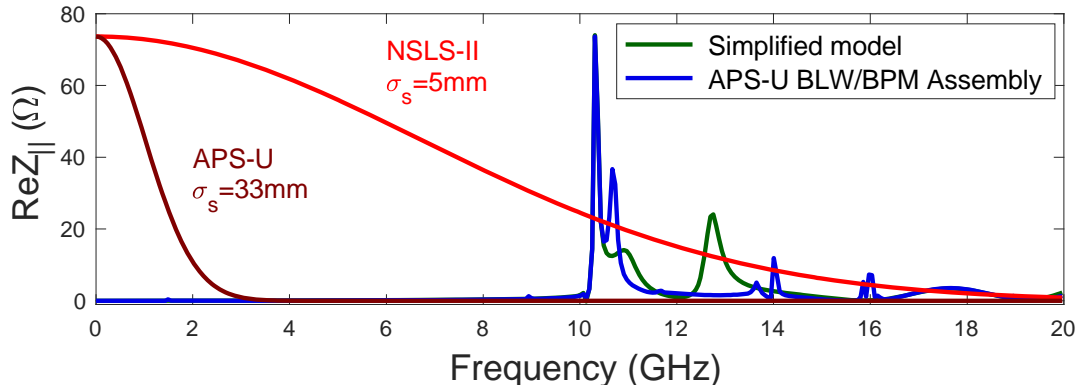


Fig. 14: The real part of the longitudinal impedance up to 20GHz.

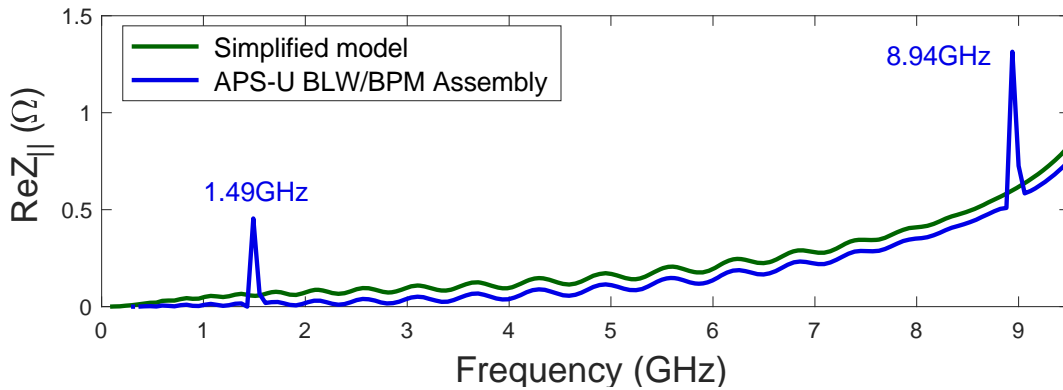


Fig. 15: The real part of the longitudinal impedance up to 9.5GHz.

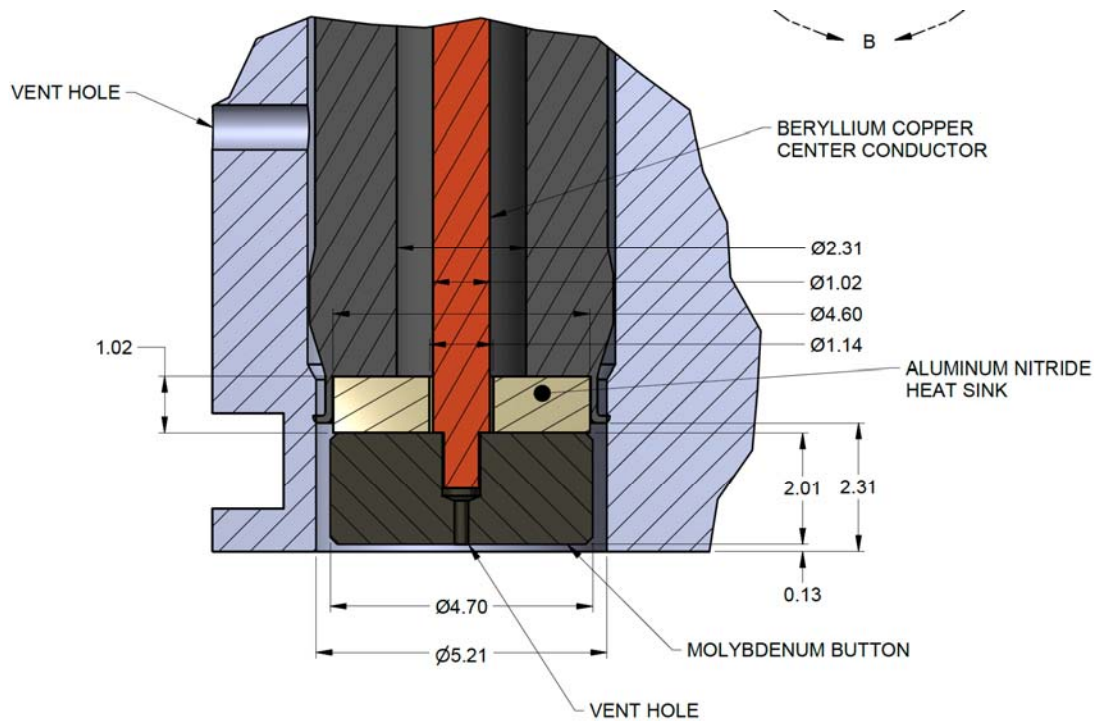


Fig. 16: The NSLS-II small aperture MPF BPM Button.

### Concluding remarks

- A complete set up was developed in NSLS-II for testing the APS-U vacuum/diagnostic components. The set up consists of the Gate Valves, Tapered Transitions for matching the NSLS-II octagonal shape of the vacuum chamber with the APS-U circular profile, diagnostic instrumentations, vacuum pumps, ... .
- The APS-U bellows/BPM assembly has been tested in the NSLS-II storage ring during three days of beam studies and it was removed before the regular operation. The average current was limited during ( $I_{av} < 100mA$ ) the beam studies due to the local overheating issues observed on the upstream side of the APS-U Bellows/BPM. Based on the measured results and on the visual inspection after the beam test, we can conclude that the RF contact fingers have a poor contact with an axial gap in the area of the RF contact spring and the BPM pipe. The present APS-U bellows design needs to be optimized to avoid the RF contact fingers fall off from the central BPM body due to the longitudinal or transverse mechanical motion. The current length of the RF contact fingers can accommodate very small increases in the overall length from the nominal installation position. Without some type of stroke limiting device or perhaps an increase in the overall length of the RF contact fingers, this problem will most likely be common during installation. It would be good to re-test the APS-U bellows/BPM assembly under the beam at high average current and in



a time interval more than 6-7 hours after all obstacles eliminations in the desing, to be sure that the localize heating issue has been resolved and the APS-U bellows/BPM assembly is safe for operation.

- The beam spectra measurements show existence of the trapped mode at low frequency. The cut-off frequency for  $H_{m1}$ -mode like in a coaxial waveguide can be defined as

$$f_c^{H_{m1}} \approx \frac{1}{\sqrt{\epsilon_r}} \frac{c}{\pi} \frac{m}{(r_1 + r_2)}, \quad (1)$$

where  $r_1$  and  $r_2$  are the radii of the inner and outer conductors,  $m=1, 2, 3, k$  and  $\epsilon_r$  is relative permittivity (dielectric constant). For the radius  $r_1 = 4mm$  and  $r_2 = 4.25mm$  and  $\epsilon_r = 1$ , the first resonant mode has a frequency  $f = 11.6GHz$ . Since the beam sees the ceramics washer, which is used for the vacuum seal and for the central pin stabilization, the relative permittivity needs to be taken into account, as it shown in Eq. (1). The APS-U BPM Button design has a coaxial cavity type in location of the ceramics washer, which is differed from the NSLS-II design (see Fig. 15). The electron beam can generate the TEM-mode like in a coaxial cavity, those frequency can be defined as

$$f = \frac{c}{\sqrt{\epsilon_r}} (p/2L), \quad (2)$$

where  $c$  is velocity of light,  $p$  is the number of field variation in  $z$ -direction,  $L$  is the cavity length. The numerical analysis in Fig. 14 shows existence of the low frequency trapped mode in the APS-U BPM Button. It needs to be confirmed by the APS-U team with detailed analysis of the longitudinal spectra using the final designed geometric parameters of the APS-U BPM Button. The present APS-U BPM Button geometry needs to be optimized from impedance point of view to reduce the risk of the low frequency modes generation.

- The experimental data shows that the outside measured APS-U bellows/BPM temperature reaches the steady state after 20 min, while in NSLS-II all vacuum components show the heat rise within 6-7 hours. It can be due to appearance of the resonance mode in location of a poor RF finger contact. It needs to be verified.
- We welcome 2<sup>nd</sup> set of tests at NSLS-II including improved APS-U Bellows/BPM assembly and the kicker stripline. We are carrying out machine modelling and tracking / beam studies to check for limitations on injection efficiency once the ring is equipped with the new chambers with small apertures.